# Numerical Simulation with Bleed and Bypass Effects of Nacelles on SST

Takeshi Kaiden (Mitsubishi Heavy Industries, Ltd.)
Makoto Shibata (Japan Aircraft Development Corporation)
Toshiyuki Iwamiya (National Aerospace Laboratory)

## Abstract

Supersonic transport is aero-designed with the consideration of the integration between airframe and engine nacelles to utilize the shock wave from them. At the high speed flight, the bleed and bypass air is blown outside from nacelle surface to prevent the flow separation at the compression surface and to control the mass flow to the engine. Therefore it is necessary to assess the aerodynamic interference by blowing. It is here reported that the aero-interference phenomena by blowing from nacelles are obtained by Navier-Stokes solver with overset grids.

## Introduction

Integration design of airframe-engine is one of the important problems on the aero-design of supersonic transport. Especially, the shock wave from engine nacelles and diverters is utilized in order to increase the lift and reduce the drag increment. As the results, larger lift to drag ratio(L/D) is realized. But the bleed and bypass air from the nacelles have to be noticed in the actual condition. On the supersonic cruise condition, the air on the intake inner wall is breathed to remove the boundary layer which induces the total pressure loss. Also, on the transonic condition, the mass flow which is coming into the intake is larger than necessary for the engine. Therefore the part of the inflow air has to be bypassed from nacelles.

The bleed and bypass air from the outside of the nacelles causes a shock wave, an expansion wave and flow separation induced by them. This phenomena is due to the aerodynamic interference with the boundary layer on the nacelle surface. It is possible to induce the decrease of the lift and the increment of the drag. Therefore it is necessary to estimate the accurate influence by blowing the bleed and the bypass air from the outside of the nacelles in order to realize the higher L/D.

If these effects are studied by wind tunnel testing, the cost of the model and the test equipments will be very expensive. It is difficult to do this by wind tunnel test in a simple manner. In the present paper, a three-dimensional thin-layer Navier-Stokes analysis code is adopted. Numerical method is based on the Chimera technique. Overset grids are used to represent the wing-body configuration of typical Supersonic Transport(SST) and the inner and the outer nacelles. The complicated flow phenomena is captured as the results of Navier-Stokes analysis.

## Condition for blowing from nacelle

For the CFD analysis of bleed and bypass effects, the boundary conditions on the nacelles wall have to be set to simulate the blowing air. The schematics of blowing from nacelles is shown in Fig.1. The bleed and bypass air in the inner side of the nacelles are discharged to the outside of them. It is noticed the exit angle for the bleed and bypass is 10 and 30 degrees, respectively.

The location of blowing and mass flow ratio for the bleed and the bypass are described in the Tab.1. Mach number and the altitude for bleed condition are 2.4 and 56,000ft. Those for bypass condition are 1.2 and 32,000ft. Mass flow ratios which are discharged for bypass air are set to 0,10,20 and 40%.

## Numerical analysis

### Grid generation

Chimera technique[1)-3)] is applied to this computation. The grids which are used in this method are generated independently for the each component. The details of this numerical procedure is described in the next section. The number of the grids used here is seen in the Tab.2. These grids are generated by the algebraic interpolation method.

The inner nacelle grid for the bleed and the bypass computation are shown in Fig.2. The grid for the bleed case has 6 slots in total. From those locations, the bleed air sucked at the cowl and the spike of the intake is blown to the outer region. On the other hand, the grid for the bypass case is generated with the consideration of slot area in accordance with 4 bypass ratios. As the bypass case is for the transonic condition, the aft-nozzle geometry has to be changed usually. Since the objective of this study is to capture the aerodynamic interference on the wing by blowing from the nacelles, the geometry of the bypass case is the same as one of the bleed case.

Fig.3 shows the overset grids with SST and the nacelles. It is possible to check the overlapping situation of these grids from this figure.

### Flow solver

The governing equations are three-dimensional thin layer Reynolds-averaged Navier-Stokes equations. The convective term is discretized using Roe's flux difference splitting with MUSCL[4)]. LU-ADI implicit method is adopted in time integration. The local time stepping is used to accelerate the convergence to the solution. The turbulence model used here is the algebraic model of Baldwin-Lomax type.

The solution process of Chimera technique is described in Fig.4. First of all, physical properties of the hole on SST are interpolated from those of the inner and outer nacelles(Process A). Hole stated here is defined as the location where the flow properties is set from those of the other grid. After the interpolation, N-S analysis on SST is performed(Process B). At this time, the grid points of the hole are not calculated. At the next step, physical properties of the hole on nacelles are interpolated from those of SST(Process C). Finally, N-S computation on nacelles are done(Process D). The hole is treated in the same manner of the SST computation. These process is repeated until the residual is converged.

Boundary conditions on the nacelles are set as follows. The flow properties at the inlets of nacelles are extrapolated from the upstream to simulate approximate flow-through nacelles in the supersonic and transonic case. Those at the outlets on the supersonic calculation are given to simulate the engine operation. But in the transonic case, free stream conditions are posed to simplify the calculation.

## Computational results

The computational flow conditions of supersonic cruise are Mach number of 2.4, angle of attack of 4.5 degrees and Reynolds number of 92 million based on the chord at the wing kink station. Those of transonic cruise are 1.2, 4.5 degrees and 138 million, respectively.

### Bleed effect

Pressure distribution when bleed air is blowing from the nacelle sides is shown in Fig.5. Compared with the case without bleed air, both results have little difference. The surface streamlines in Fig.6 give us the similar result. This is because of little mass flow ratio of bleed air and small exit angle(10 degrees) from the outer surface of nacelles. It is also recognized from the detail of flow fields near the surface at blowing in Fig.7. Therefore the bleed air gives us little interference to the wing and the forces does not changed consequently(Tab.3).

### Bypass effect

i) Flow field induced by the bypass air

Fig.8(a) shows the schematics of flow field induced by large bypass air. The boundary layer on the nacelle surface is separated by blowing the bypass air to it. As the result, the shock wave by the separation occurs at this location. The flow coming over the bypass air generates a expansion wave and the shock wave by reattachment when it is reattached to the nacelle surface. The larger is the bypass ratio, the clearer this flow pattern becomes. The pressure distribution near the exit in the case of bypass ratio 40% is presented in Fig.8(b). Though the reattached shock wave could not be confirmed because it is generated backward, the shock wave and the expansion wave by the separation are able to be seen.

ii) Influence to the flow field on the lower wing

The pressure distributions of the lower wing are shown in Fig.9. These figures indicate that the shock wave by the separation propagates more to the lower wing as the bypass ratio is larger. On the lower wing between the inner and outer nacelles, the shock waves by the separation interfere each other. From the streamlines on the lower wing in Fig.10, the flow direction is curved due to the shock wave by the bypass air.

iii) Influence to the flow field on the nacelle

The streamlines on the nacelle surface are shown in Fig.11. Red streamlines in these figures are started from the lip of the intake. Yellow ones and Pink ones are done from the bypass exit and the diverter, respectively. As the bypass ratio increases, the flow induces downward at the rear of the exit. This phenomena is due to the complicated interference stated next. The shock wave and the expansion wave induced by the bypass air on the nacelles give the influence to the lower wing, so that the pressure there becomes high. On the other hand, the suction by the expansion wave on the nacelles is dominant because the interference between the wing and nacelles is less on the lower part of the nacelles. Due to the difference of these pressure, the air coming from the diverter flow into the region between the separated boundary layer and the surface on the nacelle.

ix) Comparison with lift and drag

Tab.4 summarizes the influence of the bypass ratio to lift and drag. The lift is increasing as the bypass ratio is larger. The increment of it is proportional to the bypass ratio. This is the reason why the shock wave by the separation on the nacelles becomes strong and it makes the compression on the lower wing. The drag is also increasing as well as the lift. But the increment of it is smaller than expected and it is only 2counts in the maximum case. It is supposed that the shock wave by the bypass air makes the compression region on the rear of the lower wing and that the thrust component is generated on the wing.

## Conclusion

Navier-Stokes analysis including the bleed and bypass effect is conducted and the aerodynamic interference between SST and nacelles is captured.

It is found that the bleed air in this study gives little impact to the flow field around SST and nacelles. Also, it is obtained that the shock wave generated by the bypass air increases the lift and the drag as the result of the complicated interference. The increment of lift and drag is about 1.0% and 0.5% per 10% bypass air, respectively.

It is necessary to evaluate these numerical results quantitatively by wind tunnel tests as future action.

## Acknowledgment

The greater part of the work was performed under contract of Ministry of International Trading Industry, The Society of Japanese Aerospace Companies, Inc. Authors wish to thank BCAG(Boeing Commercial Airplane Group), for the permission to use the configuration data of the SST and the nacelle and to publish the results.

## References

(1) NASA Ames Space Shuttle Flow Simulation Group, Buning, P., Chiu, I., Martin, F., Meakin, R., Obayashi, S., Rizk, Y., Steger, J., and Yarrow, M., "Numerical Simulation of the Integrated Space Shuttle Vehicle in Ascent," 4th internat. Conf. on Super Computing, Santa Clara, Calif., April, 1989.
(2) Kaiden, T. and Tamura, Y.,"Time Accurate Numerical Simulation of Separation between H-II and SRB," 5th ISCFD-Sendai, Aug., 1993
(3) Maekawa, S., Iwamiya, T., Tuboi, N. and Kaiden, T.,"CFD Analysis of SST with Nacelles," 34th Airplane Symposium in Japan, Nov., 1996(in Japanese)
(4) Fujii, K. and Obayashi, S.,"High-Resolution Upwind Scheme for Vortical Flow Simulations," J. Aircraft, Vol.26, No.12, Dec., 1989 pp.1123-1130.

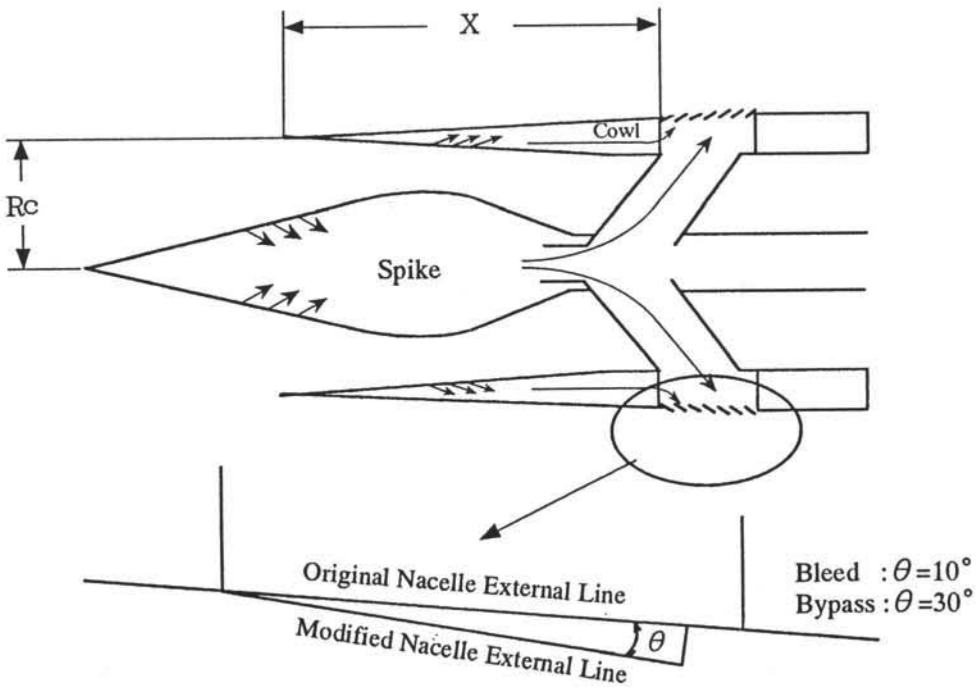


Fig.1 Schematics of blowing from nacelles

Tab.1 Condition for blowing from nacelles

Bleed condition

| Suction | Spike | | Cowl | | | |
|---|---|---|---|---|---|---|
| Location (X/Rc) | 5.6 | 5.8 | 3.225 | 3.425 | 3.625 | 3.935 |
| Mass flow ratio(m/mc) | 0.97% | 0.82% | 0.31% | 0.37% | 0.46% | 1.20% |

Bypass condition

| | | | | |
|---|---|---|---|---|
| Location (X/Rc) | – | 3.38～3.68 | 3.38～3.97 | 3.38～4.56 |
| Mass flow ratio(m/mc) | 0 | 10% | 20% | 30% |

*) mc : Engine mass flow at cruise
m : Bleed or bypass mass flow

## Tab.2 Number of the grid points

### For bleed

| | Grid points for each direction | | | Total grid points |
|---|---|---|---|---|
| | Streamwise | Circumferential | Radial | |
| SST | 135 | 155 | 63 | 1,318,275 |
| Inner nacelle | 141 | 85 | 50 | 599,250 |
| Outer nacelle | 141 | 85 | 50 | 599,250 |
| (Total) | | | | 2,516,775 |

### For bypass

| | Grid points for each direction | | | Total grid points |
|---|---|---|---|---|
| | Streamwise | Circumferential | Radial | |
| SST | 135 | 155 | 63 | 1,318,275 |
| Inner nacelle | 128 | 85 | 50 | 544,000 |
| Outer nacelle | 128 | 85 | 50 | 544,000 |
| (Total) | | | | 2,406,275 |

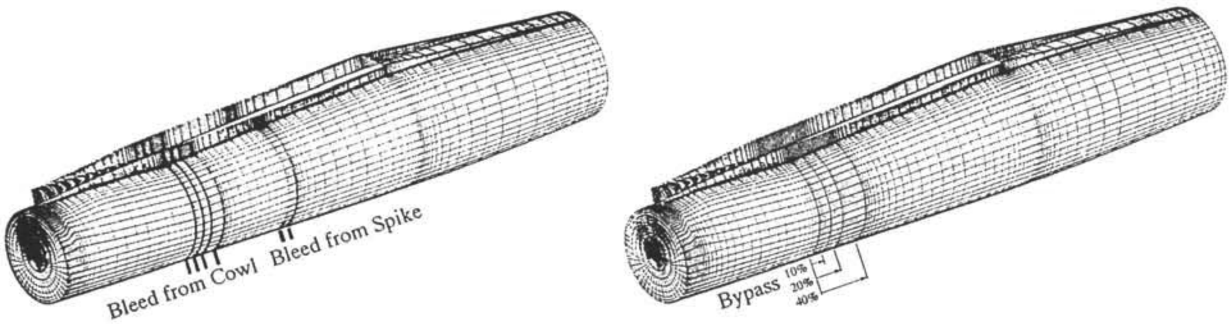


For bleed　　For bypass

Fig.2 Nacelle grid

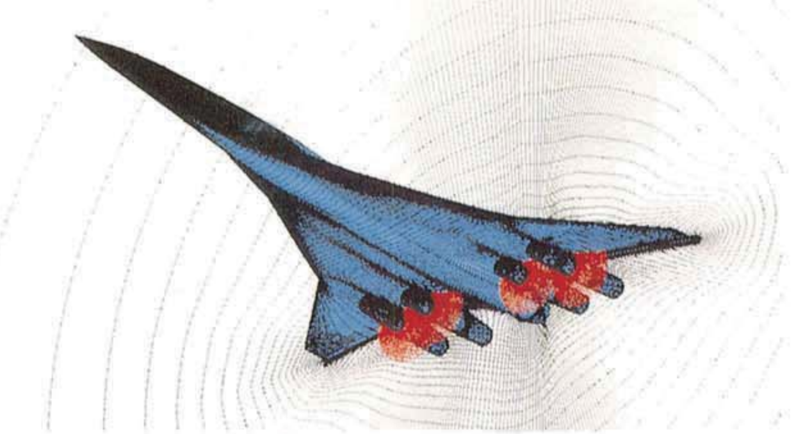

Fig.3 Overset grids

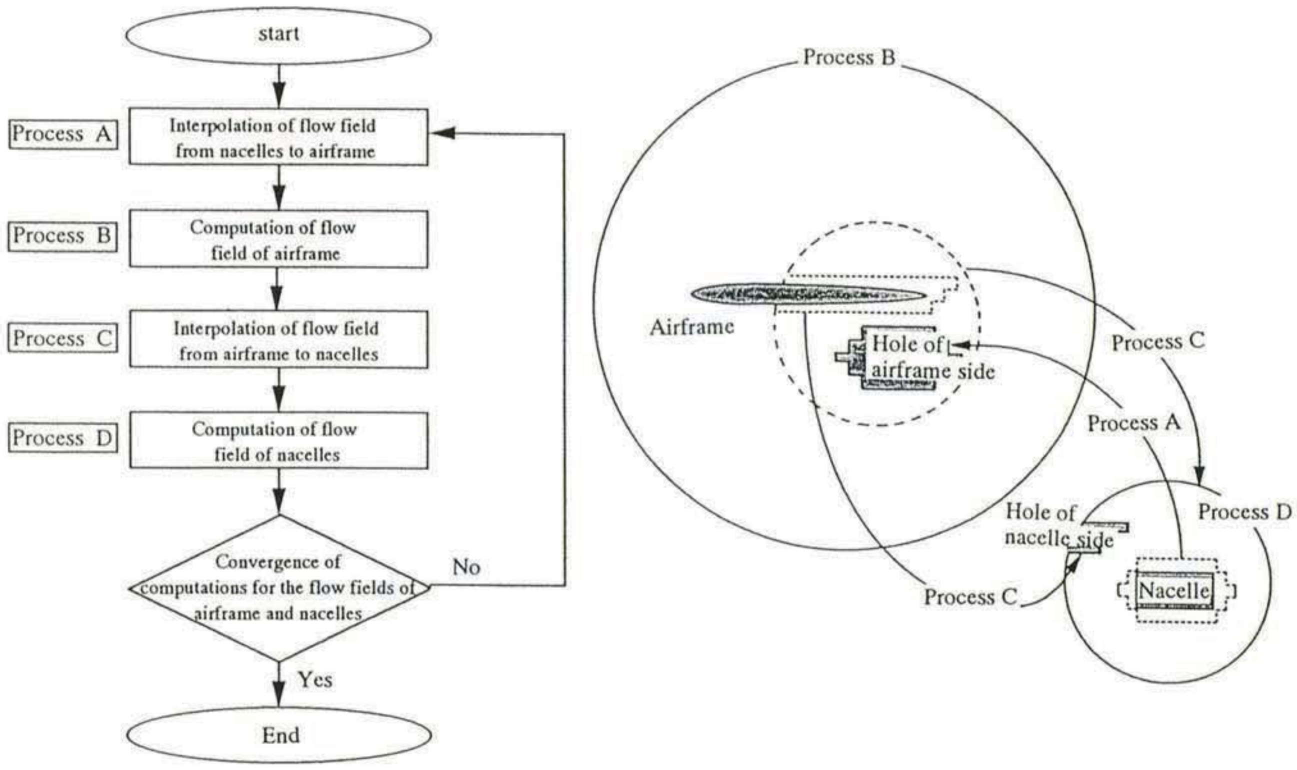


Fig.4 Flow chart for computation

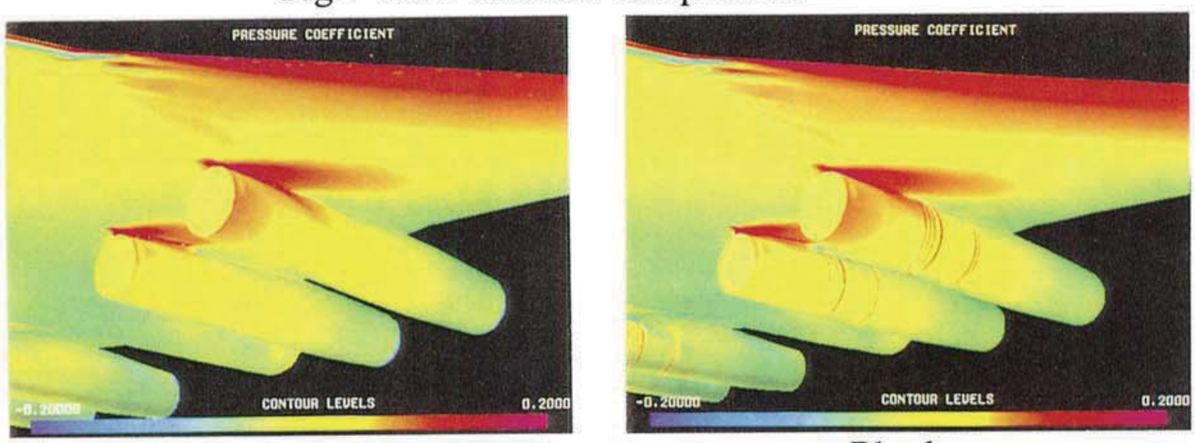


Bleed off Bleed on

Fig.5 Surface pressure contour near nacelles

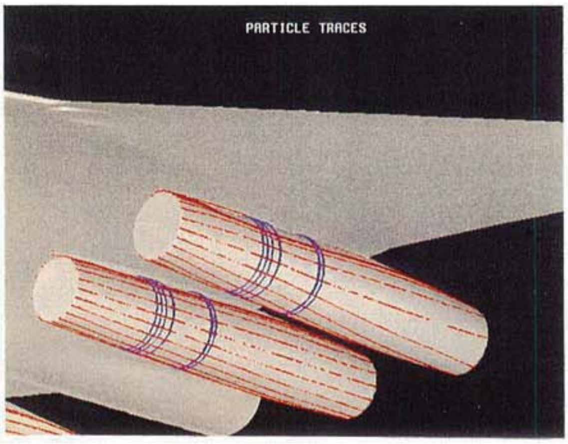


Fig.6 Surface streamlines on nacelles (bleed case)

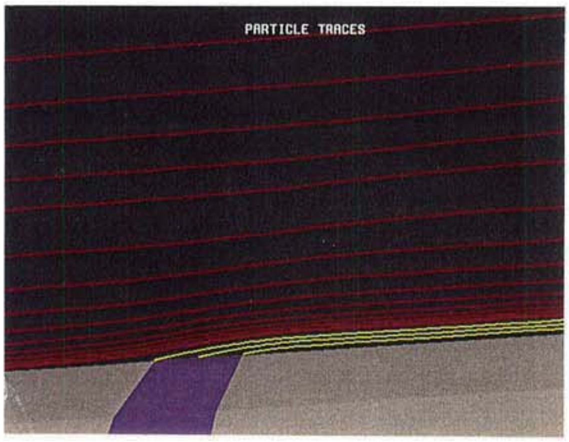


Fig.7 Closed-up streamlines around bleed region

Tab. 3 Bleed effect

| | | Bleed off | Bleed on | Difference |
|---|---|---|---|---|
| CL | Wing-Body | 0.08263 | 0.08291 | 0.00028 |
| | Nacelles | 0.00076 | 0.00075 | -0.00001 |
| | Total | 0.08339 | 0.08366 | 0.00027 |
| CD | Wing-Body | 0.00801 | 0.00801 | 0.00000 |
| | Nacelles | 0.00097 | 0.00093 | -0.00004 |
| | Total | 0.00898 | 0.00894 | -0.00004 |

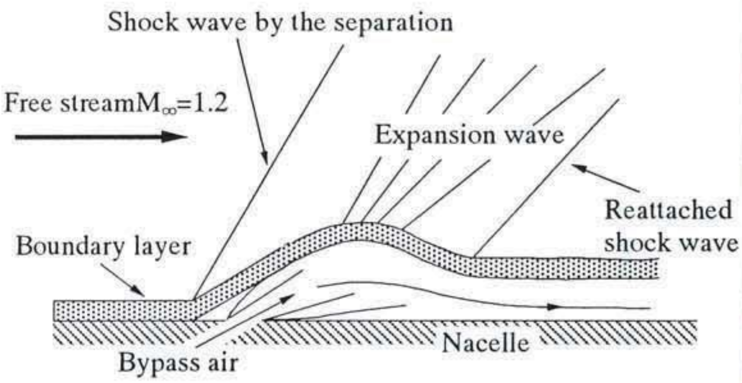


(a) Schematics of flow field

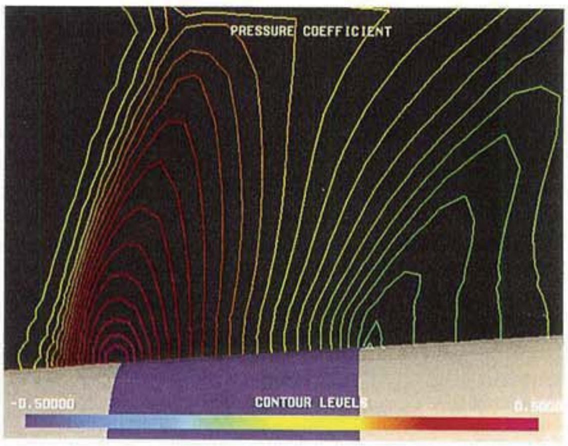


(b) Pressure distribution

Fig.8 Flow field near bypass region (bypass ratio 40%)

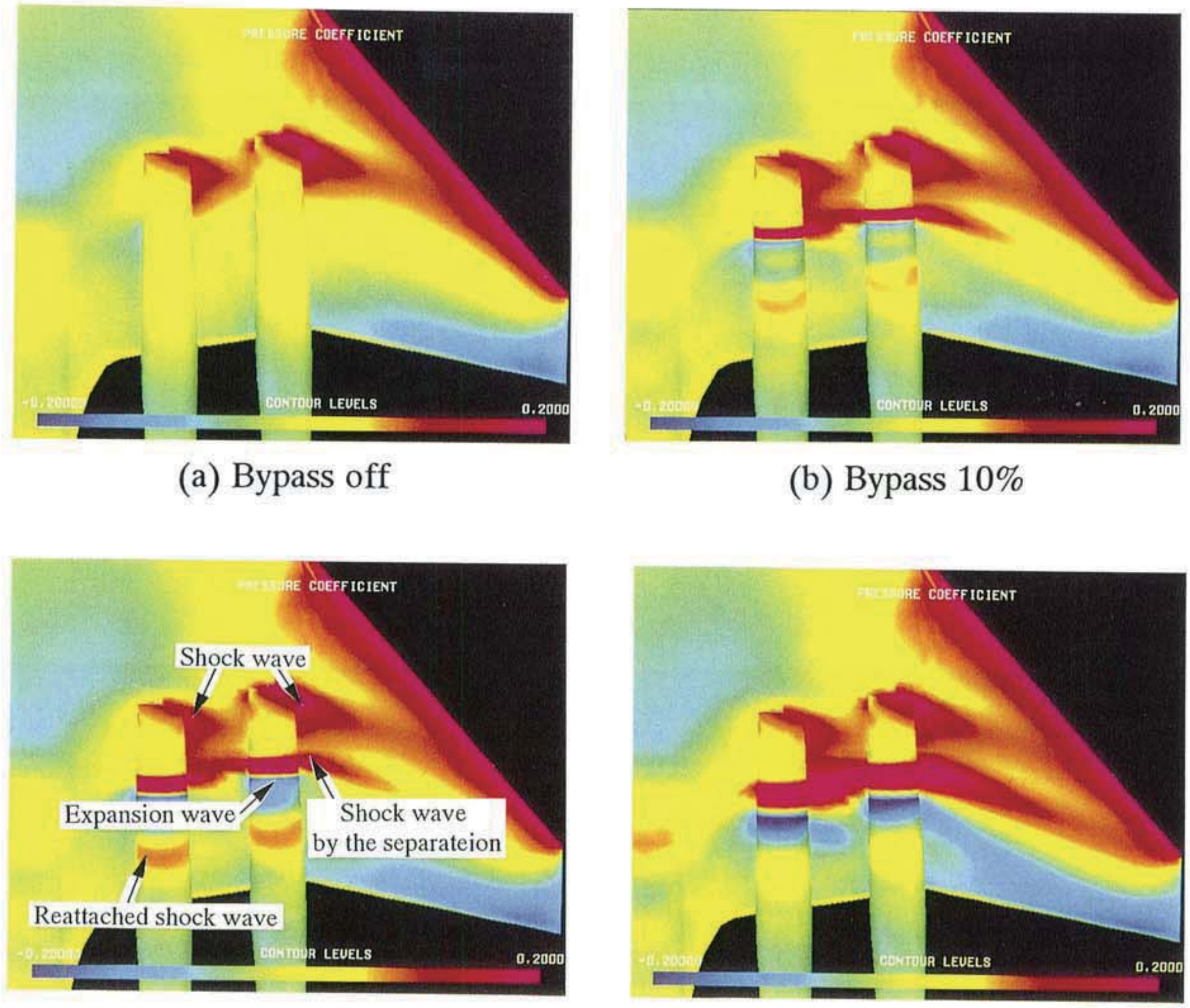


(a) Bypass off (b) Bypass 10%

(c) Bypass 20% (d) Bypass 40%

Fig.9 Surface pressure contour near nacelles (bypass case)

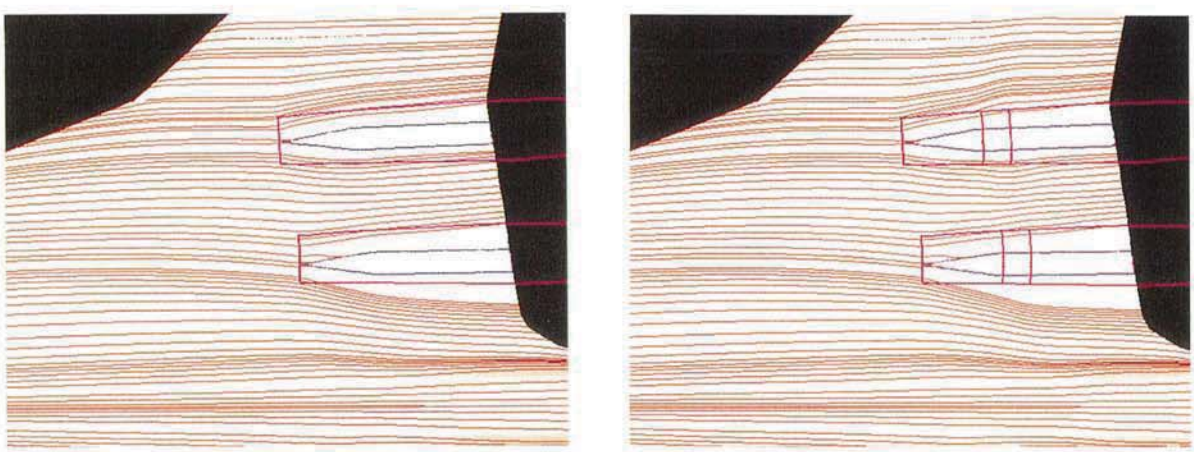

(a) Bypass off (b) Bypass 40%

Fig.10 Surface streamlines on lower wing surface

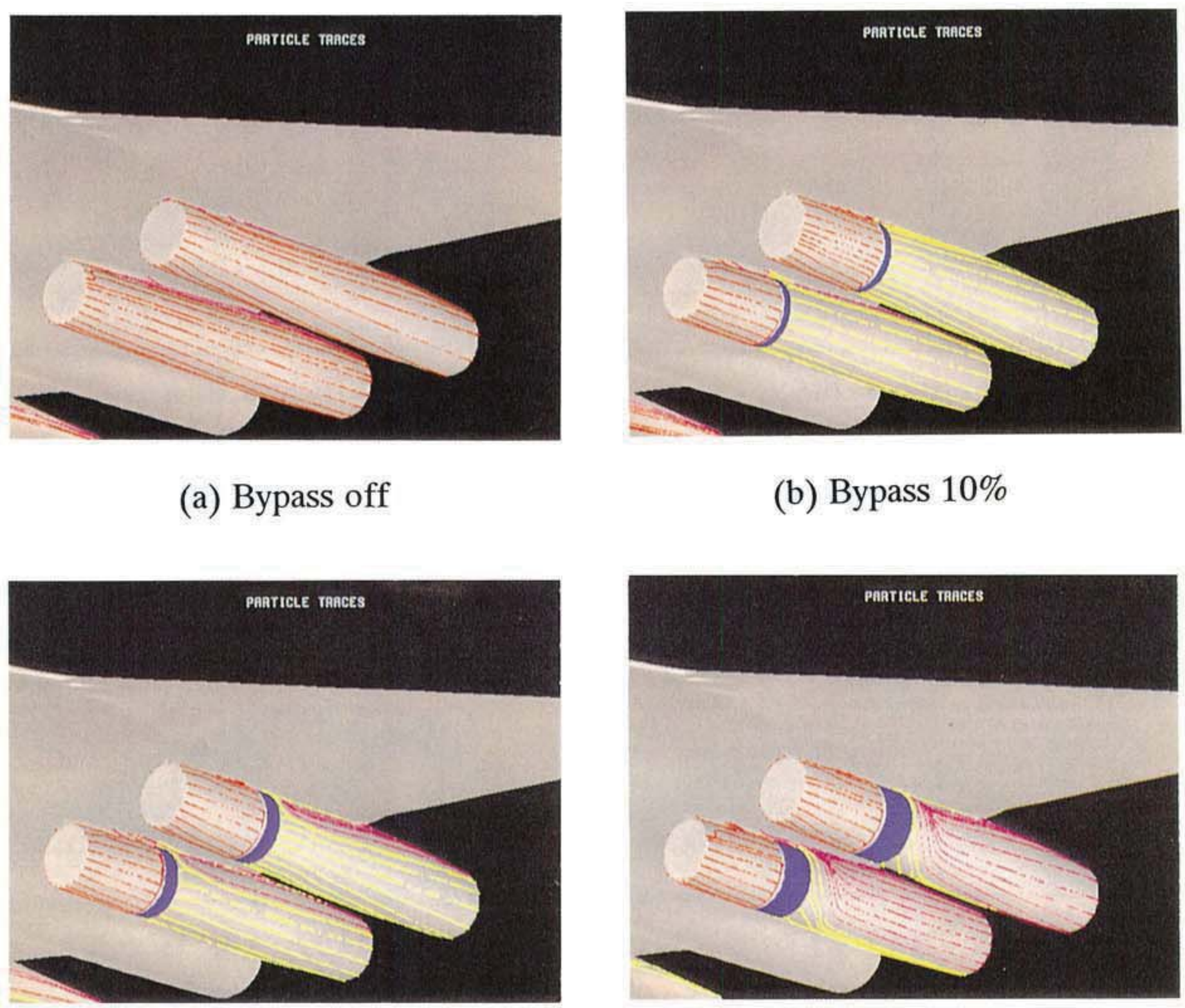


(a) Bypass off　(b) Bypass 10%

(c) Bypass 20%　(d) Bypass 40%

Fig.11 Surface streamlines on nacelles (bypass case)

Tab.4 Bypass effect

| | | Bypass off | Bypass 10% | Bypass 20% | Bypass 40% |
|---|---|---|---|---|---|
| $C_L$ | Wing-Body | 0.13420 | 0.13558 | 0.13689 | 0.13957 |
| | Nacelles | 0.00075 | 0.00087 | 0.00089 | 0.00100 |
| | Total | 0.13495 | 0.13643 (+1.1% ) | 0.13778 (+2.1% ) | 0.14057 (+4.2% ) |
| $C_D$ | Wing-Body | 0.00761 | 0.00769 | 0.00771 | 0.00775 |
| | Nacelles | 0.00094 | 0.00090 | 0.00092 | 0.00095 |
| | Total | 0.00855 | 0.00859 (+0.5% ) | 0.00863 (+0.9% ) | 0.00870 (+1.8% ) |